

Critical size for exchange bias in ferromagnetic-antiferromagnetic particles

A. N. Dobrynin, D. N. Ievlev, K. Temst, and P. Lievens^{a)}

Laboratorium voor Vaste-Stoffysica en Magnetisme, K.U.Leuven, Celestijnenlaan 200D, B-3001 Leuven, Belgium

J. Margueritat, J. Gonzalo, and C. N. Afonso

Instituto de Optica, CSIC, Serrano 121, 28006 Madrid, Spain

S. Q. Zhou and A. Vantomme

Instituut voor Kern- en Stralingsfysica, K.U.Leuven, Celestijnenlaan 200D, B-3001 Leuven, Belgium

E. Piscopiello and G. Van Tendeloo

Elektronenmicroscopie voor Materiaalonderzoek, Universiteit Antwerpen, Groenenborgerlaan 171, B-2020 Antwerp, Belgium

(Received 28 February 2005; accepted 23 May 2005; published online 27 June 2005)

We present a study of the magnetic properties of oxidized Co nanoparticles with an average grain size of 3 nm, embedded in an amorphous Al₂O₃ matrix. These nanoparticles can be considered as imperfect Co-core CoO-shell systems. Magnetization measurements after magnetic field cooling show a vertical shift of the hysteresis loop, while no exchange bias is observed. With a simple model, we show that there is a critical grain size for hybrid ferromagnetic-antiferromagnetic particles, below which exchange bias is absent for any ratio of ferromagnetic and antiferromagnetic constituents. The reason is that the interfacial exchange energy dominates over other energies in the system due to a large surface-to-volume ratio in the nanoparticles. © 2005 American Institute of Physics. [DOI: 10.1063/1.1978977]

When a ferromagnetic-antiferromagnetic (FM-AFM) system is cooled down in an external magnetic field through the Néel temperature of the antiferromagnet, the magnetic hysteresis loop is shifted along the field axis, a phenomenon known as exchange bias (EB).¹⁻⁴ A simple model for EB was proposed by Meiklejohn and Bean.¹ Before cooling down, the AFM part is in a paramagnetic state and its magnetic moments can be aligned by an external field. When cooling down through the Néel temperature, the AFM structure is established with AFM spins parallel to FM spins. The interfacial AFM spins tend to align collinearly with the FM spins. Since the AFM structure does not rotate in a magnetic field, this collinear interfacial spin alignment creates a unidirectional anisotropy, such that it is harder to rotate FM spins in one direction than in the opposite one. Although knowledge on the FM-AFM interface structure is crucial for the understanding of EB in particular systems, all present approaches assume that only interfacial exchange interactions cause the EB.²⁻⁴ Therefore, in practice, one can consider an empirical interfacial exchange energy directly proportional to the FM-AFM interface area.

Hybrid FM-AFM nanoparticles (NPs) offer the opportunity to study EB at the nanoscale. Apart from the fundamental interest, this is important for applications: asymmetric exchange-biased loops are used in spin valves, and exchange anisotropy helps to overcome the superparamagnetic limit.⁵

In this letter, we compare the magnetic properties of pure Co and oxidized Co NPs embedded in an amorphous Al₂O₃ matrix. The samples were prepared by alternated pulsed-laser deposition.^{6,7} An ArF excimer laser (fullwidth at half-maximum of the pulse=20 ns, repetition rate=20 Hz), with an average energy density of 1.9 J/cm², was sequentially

focused on the surface of high-purity Al₂O₃ and Co rotating targets. The films were grown in vacuum ($p < 10^{-7}$ mbar) on amorphous SiO₂ substrates at room temperature, and placed 32 mm away from the target surface. The deposition sequence was the following: a 10 nm thick amorphous Al₂O₃ layer was grown, followed by a submonolayer of Co NPs. This sequence was repeated five times, and finally a protective Al₂O₃ layer was deposited. In the case of the sample containing oxidized Co NPs a pulsed gas valve was used to introduce a transient dynamical O₂ pressure for 20 s into the deposition chamber after the growth of each layer of Co NPs. The O₂ peak pressure was about 7×10^{-4} mbar. Both samples, containing pure and oxidized Co NPs, respectively, were prepared using identical experimental conditions apart from the oxidation step. While the exact structure of the oxidized NPs is unknown, they can be considered as consisting of a pure Co core and an incomplete CoO shell.

Rutherford backscattering spectrometry (RBS) was used to determine the content of Co in the samples using a 1.57 MeV He⁺ beam. Figure 1(a) shows an RBS spectrum for the nonoxidized sample in which the peaks corresponding to the individual layers of Co NPs are observed. Such a "fine structure" means that interlayer diffusion is not a significant process. Intensities of the Co peaks are approximately equal, meaning that the amount of Co is about the same for each layer of NPs. The morphology of the produced NPs was characterized by transmission electron microscopy (TEM) using films with a sandwich structure (Al₂O₃/Co NPs/Al₂O₃) deposited on carbon-coated mica substrates under the same conditions as the samples used for the magnetization studies. Figure 1(b) shows a plan view of a sample containing pure Co NPs. Most of the NPs are spherical, they are well separated from each other, and their mean size is about 3 nm.

^{a)}Electronic mail: Peter.Lievens@fys.kuleuven.be

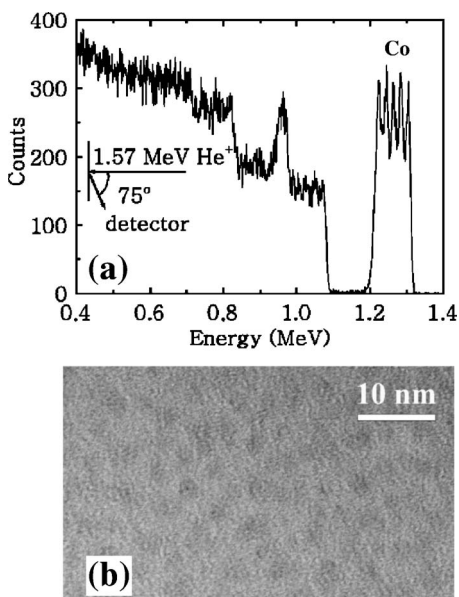


FIG. 1. (a) RBS spectrum of the nonoxidized sample: five Co peaks are resolved and correspond to the different layers of Co NPs. The backscattering geometry is shown in the inset. (b) TEM: plan view image of Co NPs in Al_2O_3 matrix.

Magnetization measurements were performed with vibrating sample and superconducting quantum interference magnetometries at 5 K in magnetic fields up to 10^4 Oe. In Fig. 2(a) the hysteresis loops for zero-field cooling (ZFC) from room temperature for the nonoxidized and oxidized samples are compared. The magnetization values are normalized according to the amount of Co in the samples. Hysteresis loops after field cooling (FC) in a field of 10^4 Oe were also measured. For the nonoxidized sample there is no difference between ZFC and FC loops. For the oxidized sample the FC loop differs from the ZFC loop only by a shift along the magnetization axis, as shown in Fig. 2(b). The ZFC loop is invariant with respect to coordinates' inversion. This perfect symmetry proves the absence of exchange biased NPs in the sample, since otherwise asymmetric steps or different magnetization reversal slopes for the right and left parts of the hysteresis loop would be observed. The saturation magnetization of the oxidized sample is smallest due to the AFM CoO part with zero net magnetic moment. The coercivity of the oxidized sample is significantly larger: 1050 Oe versus 400 Oe for the nonoxidized one.

The magnetic behavior of the FM-AFM hybrid systems in an external magnetic field is essentially governed by the competition between four energy terms: the Zeeman energy of the ferromagnet (E_Z), the anisotropy energy of the FM

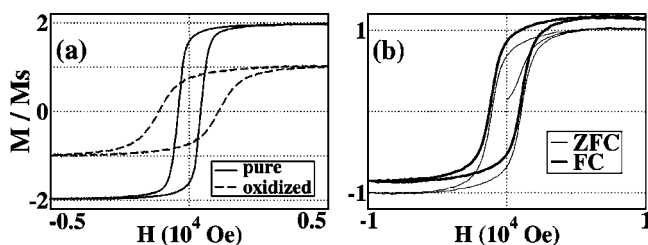


FIG. 2. (a) ZFC to 5 K for nonoxidized and oxidized samples; (b) ZFC and FC to 5 K for the oxidized sample. Magnetizations are normalized on amount of Co in the samples; the saturation magnetization of the oxidized sample is taken as unity.

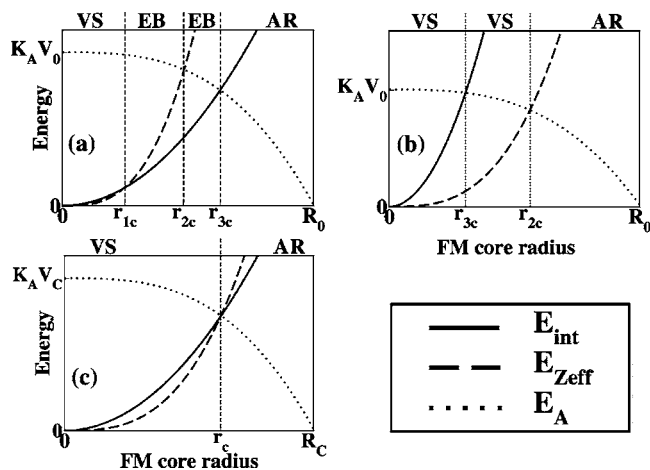


FIG. 3. E_{int} , E_A , and $E_{Z_{\text{eff}}}$ as functions of the FM core radius. (a) “Large” particles: exchange bias is possible; (b) “Small” particles: exchange bias is denied; (c) critical case. The following radii are indicated here: r_{1c} —when $E_{Z_{\text{eff}}} = E_{\text{int}}$; r_{2c} —when $E_{Z_{\text{eff}}} = E_A$; r_{3c} —when $E_{\text{int}} = E_A$; r_c —when all energies are equal.

(E_F) and of the AFM (E_A) parts, and the exchange energy at the FM-AFM interface (E_{int}). The AFM only feels the applied magnetic field via the exchange interaction with FM spins at the interface. Here we assume that the applied fields stay well below the AFM spin-flop field. Weak dipole-dipole interactions are not taken into account. The magnetic domain structure also is not considered since the small particles are single domain.⁸

In order to rotate the FM spins, the Zeeman energy shall first overcome the FM anisotropy energy barrier. It is convenient to introduce an effective Zeeman energy $E_{Z_{\text{eff}}} = |E_Z| - |E_F|$ (here and further we will consider only maximal absolute values of the energies, such that $E_A \equiv |E_A|$ and $E_{\text{int}} \equiv |E_{\text{int}}|$). Further $E_{Z_{\text{eff}}}$ competes with E_{int} . If $E_{Z_{\text{eff}}} > E_{\text{int}}$, there are two possibilities. First, when $E_{\text{int}} < E_A$, the FM spins will be rotated while AFM spins will not, and EB will be observed. In the second case of $E_{\text{int}} > E_A$, there will be no EB. AFM spins will be rotated coherently with the FM spins, as was shown for FM-AFM bilayers,⁹ and coercivity will be larger than that for a pure FM particle of the same size. For the case of $E_{Z_{\text{eff}}} < E_{\text{int}}$ there are two possibilities as well. First, when $E_{Z_{\text{eff}}} < E_A$, the Zeeman energy is not enough either to overcome the interfacial energy barrier or to rotate the AFM spins. The FM part will stay “frozen” in an external field, and after the field cooling, this will show up as a vertical magnetization shift. In the second case of $E_{Z_{\text{eff}}} > E_A$, the Zeeman energy is enough to rotate both FM and AFM spins. Thus, there are three possible states in the system: EB, when $E_{\text{int}} < E_{Z_{\text{eff}}}$ and $E_{\text{int}} < E_A$; AFM spin rotation (AR), when $E_A < E_{\text{int}}$ and $E_A < E_{Z_{\text{eff}}}$; and “frozen” FM state, leading to the vertical shift (VS) after the field cooling, for the case of $E_{Z_{\text{eff}}} < E_{\text{int}}$ and $E_{Z_{\text{eff}}} < E_A$.

For an ideal spherical FM core-AFM shell system with radius R_0 and FM core radius r , the energies can be written as $E_{\text{int}} = 4\pi\sigma r^2$, with σ an empirical exchange coupling constant; $E_A = 4\pi K_A (R_0^3 - r^3)/3$, where K_A is the volume anisotropy constant of the antiferromagnet; $E_{Z_{\text{eff}}} = (4\pi r^3 \epsilon_Z)/3$, with the energy density $\epsilon_Z(H) = (\mu_F H - K_F)$, μ_F is a specific magnetic moment, K_F a volume anisotropy constant of the FM part, and H the applied magnetic field. In Fig. 3, the

energies are plotted as a function of the FM core radius. In Fig. 3(a) the case of “large” particles is presented. All three cases (VS, EB, and AR) can be realized at different ratios of FM to AFM in the particle. The case of “small” particles is plotted in Fig. 3(b). Here the conditions for EB are never fulfilled since the E_{int} is always larger than $E_{Z_{\text{eff}}}$. The critical case for EB to occur is shown in Fig. 3(c), and the critical radius is $R_c = (3\sigma/\epsilon_Z)(1 + \epsilon_Z/K_A)^{1/3}$. An estimate for the Co/CoO case can be made with $\sigma = 3 \text{ erg/cm}^2$,¹⁰ $K_A = 2.7 \times 10^8 \text{ erg/cm}^3$,³ and $K_F = 2 \times 10^6 \text{ erg/cm}^3$.¹¹ This yields a grain size $2R_c = 12 \text{ nm}$ for a field of 10^4 Oe , well above the mean size of the NPs considered. It is important to note that the energy dependencies in the model expressions used here may deviate from quadratic and cubic laws. Nevertheless, the surface/interface-related energy will follow a power law of grain size weaker than the volume-related energy. Therefore, this would not hamper the qualitative explanation of the observed magnetization behavior.

That no EB was found after the field cooling is due to the fact that below a critical size, the exchange energy at the FM-AFM interface never can be smaller than both the effective Zeeman energy of the ferromagnet and the anisotropy energy of the antiferromagnet. Moreover, there are two regimes that coexist in the investigated hybrid FM-AFM NP systems. While the overall size is well controlled, the oxidation process may not be, resulting in homogeneously sized NPs with different ratios of FM and AFM parts. For the NPs with a smaller AFM part, the AFM spins rotate coherently with the FM spins, resulting in the observed symmetric hysteresis loop. If the FM part is small enough, it stays pinned to the AFM part in an applied magnetic field, showing up as the vertical magnetization shift in our measurements. This shift cannot be ascribed solely to the uncompensated AFM spins at the FM-AFM interface, which were shown to be the reason for EB in some systems.^{3,12} In our case those spins either rotate or stay immobile together with the FM and the rest of the AFM parts. If only AFM uncompensated spins were responsible for the observed vertical shift, this would imply a rotation of the ferromagnet with respect to the antiferromagnet, leading to EB, which is not observed.

The EB vanishing below a certain particle size resembles the disappearance of the hysteresis loop shoulders in exchange-spring multilayers and nanocomposites on small length scales.^{13,14} Such systems undergo a transition from a noncooperative to a cooperative regime, due to the interfacial exchange energy dominating the volume-proportional Zeeman energy. This is the consequence of a large surface-to-volume ratio, similar to our case.

The authors thank J. Nogués for useful discussions, and M. J. Van Bael and W. Vinckx for superconducting quantum interference device measurements. One of the authors (J.M.) acknowledges an I3P fellowship from the CSIC and the European social fund. This work is supported by the Fund for Scientific Research—Flanders (FWO), the Flemish Concerted Action (GOA/2004/02), the Belgian Interuniversity Poles of Attraction (IAP/P5/01), and the European Community’s Human Potential NanoCluster (HPRN-CT-2002-00328) programs. K.T. is a Postdoctoral Fellow of the FWO.

¹W. H. Meiklejohn and C. P. Bean, *Phys. Rev.* **102**, 1413 (1956).

²J. Nogués and I. K. Schuller, *J. Magn. Magn. Mater.* **192**, 203 (1999).

³A. E. Berkowitz and K. Takano, *J. Magn. Magn. Mater.* **200**, 552 (1999).

⁴M. Kiwi, *J. Magn. Magn. Mater.* **234**, 584 (2001).

⁵V. Skumryev, S. Stoyanov, Y. Zhang, G. Hadjipanayis, D. Givord, and J. Nogués, *Nature (London)* **423**, 850 (2003).

⁶J. M. Ballesteros, R. Serna, J. Solis, C. N. Afonso, A. K. Petford-Long, D. H. Osborne, and R. F. Hauglund, Jr., *Appl. Phys. Lett.* **71**, 17 (1997).

⁷N. M. Dempsey, L. Ranno, D. Givord, J. Gonzalo, R. Serna, G. T. Fei, A. K. Petford-Long, R. C. Doole, and D. E. Hole, *J. Appl. Phys.* **90**, 6268 (2001).

⁸R. Skomski, *J. Phys.: Condens. Matter* **15**, R841 (2003).

⁹M. S. Lund, W. A. A. Macedo, K. Liu, J. Nogués, Ivan K. Schuller, and C. Leighton, *Phys. Rev. B* **66**, 054422 (2002).

¹⁰B. H. Miller and E. D. Dahlberg, *Appl. Phys. Lett.* **69**, 3932 (1996).

¹¹M. Jamet, W. Wernsdorfer, C. Thirion, D. Mailly, V. Dupuis, P. Mélinon, and A. Pérez, *Phys. Rev. Lett.* **86**, 4676 (2001).

¹²H. Ohldag, A. Scholl, F. Nolting, E. Arenholtz, S. Maat, A. T. Young, M. Carey, and J. Stöhr, *Phys. Rev. Lett.* **91**, 017203 (2003).

¹³Eric E. Fullerton, J. S. Jiang, and S. D. Bader, *J. Magn. Magn. Mater.* **200**, 392 (1999).

¹⁴H. Zeng, J. Li, J. P. Liu, Z. L. Wang, and S. Sun, *Nature (London)* **420**, 395 (2002).